A&A 370, 436–446 (2001)
DOI: 10.1051/0004-6361:20010258

Astronomy & Astrophysics

Open clusters in the third galactic quadrant

I. Photometry

A. Moitinho[⋆,⋆⋆]

[1] Observatorio Astronómico Nacional, UNAM, Apdo. Postal 877, CP 22800, Ensenada B.C., México
[2] Instituto de Astrofísica de Andalucía (CSIC), Apdo. 3004, 18080 Granada, Spain

Received 13 December 2000 / Accepted 14 February 2001

Abstract. We have performed a photometric survey of open clusters in the third Galactic quadrant in order to study the star formation history and spatial structure in the Canis Major-Puppis-Vela region. In this paper we describe a catalogue of CCD *UBVRI* photometry of approximately 65 000 stars in the fields of 30 open clusters. The data were obtained and reduced using the same telescope, the same reduction procedures, and the same standard photometric system, which makes this catalogue the largest homogeneous source of open cluster photometry so far. In subsequent papers of this series, colour-colour and colour-magnitude diagrams will be presented which, amongst other uses, will allow the determination of an homogeneous set of cluster reddenings, distances, and ages that will constitute the observational basis for our studies of the spatial structure and star formation history in the third Galactic quadrant.

Key words. techniques: photometric – stars: fundamental parameters – Galaxy: open clusters and associations: general – Galaxy: structure – ISM: dust, extinction

1. Introduction

Open clusters are ideal objects for the investigation of several astrophysical problems, since they are groups of stars placed at a common distance, which were formed under the same conditions, in most cases at approximately the same time, and spanning a broad range in mass. These properties allow open cluster distances and ages to be better determined than in the case of isolated stars. Indeed, there is a virtually endless list of literature on stellar clusters used as tests for stellar evolution theories, and as probes of Galactic structure and evolution.

In the case of Galactic structure studies the existing compilations of open cluster parameters have allowed some understanding of the structure and development of the Galactic disc (Vogt & Moffat 1972; Janes & Adler 1982; Alfaro et al. 1991; Twarog et al. 1997; Carraro et al. 1998). However, many of the conclusions drawn from open cluster data have been if not controversial, at least affected by considerable uncertainty. Among the reasons for this situation are the lack of homogeneity of derived open cluster fundamental parameters (reddening, distances, ages, metalicities), as well as the small number of studies of certain kinds of clusters (e.g. old clusters and distant clusters).

The Catalogue of Open Cluster Data (COCD) (Lyngå 1981, 1987), which includes information for 1151 clusters (distances for 422) has been the observational basis for many Galactic structure studies. However, the parameters presented in the COCD were derived by different authors using a variety of instrumentation, techniques, calibrations, and analytic criteria, and therefore result in a rather inhomogeneous set. An analysis of the precision expected due to the effects of these inhomogeneities has been performed by Janes & Adler (1982) who have found a typical difference of 0.55 mag in distance moduli determined in different *UBV* photometric studies. But even this large scatter in distance modulus determinations might be underestimated since several clusters have much larger ranges in their estimated distances. Cases like NGC 2453 which has distance estimates from 1500 to 5900 pc are not rare. These problems have been known to the astronomical community for a long time and have led to several attempts to produce more consistent sets of open cluster parameters. Loktin & Matkin (1994) reanalysed *UBV* photometry of 330 clusters and obtained a more homogeneous, although less numerous, catalogue of open cluster reddenings, distances and ages. However, Loktin & Matkin (1994) used three different sets of isochrones in

⋆ e-mail: andrem@astrosen.unam.mx
⋆⋆ Visiting astronomer, Cerro Tololo Inter-American Observatory. CTIO is operated by AURA, Inc., under contract to the National Science Foundation.

their age and distance determinations which is likely to affect the internal precision of the catalogue. More recently, Dambis (1998) has given another contribution towards an homogeneous set of cluster parameters by redetermining the reddenings, distances and ages of 203 open clusters, younger than $\log t < 8.2$ to avoid chemical composition effects, using a single set of isochrones and an empirical ZAMS.

Although the works of Loktin & Matkin (1994) and Dambis (1998) have generated improved sets of cluster parameters by using the same kind of data (*UBV* photometry), and were analysed in an homogeneous fashion, at least two effects still contribute to degrade the precision of their results. The first one is that both works used *UBV* data from different sources, nominally on the *UBV* system but in fact were calibrated using various sets of standard stars which can produce considerably different photometry (see Table 8 in this paper, and also Bessel 1995 for a detailed comparison of some versions of the *UBVRI* system). The second and perhaps most important factor is the effect of photometric depth. Photoelectric photometry is usually limited to $V \sim 16$ mag, which in many cases is not enough for reliable distance determinations: evolutionary effects will produce redder colours and lead to underestimated distances. Also, for the younger clusters, the nearly vertical shape of the upper main sequence will introduce large uncertainties in distance determinations via ZAMS fitting.

In the light of the above mentioned problems with the current open cluster parameter compilations and of our interest in studying the star formation history and spatial structure of the Canis Major-Puppis-Vela region, we have performed a deep CCD *UBVRI* photometric survey of open clusters using the same instruments, reduction methods and standard stars. In this paper we describe the photometric database. Reddenings, distances and ages will be determined in forthcoming papers using the same Zero Age Main Sequence (ZAMS) and evolutionary models.

In the next sections we describe the observations and data reductions, and present the photometric database. Later, in Sect. 6 a comparison with previously published photometry is shown. Finally, Sect. 7 is a discussion of the interstellar extinction law in the direction of our sample.

2. Observations

Open clusters in the galactic range $217° < l < 260°$ and $-5° < b < 5°$, with angular diameters of approximately $5'$ and with estimated ages lesser than $1.3\ 10^8$ yr ($\log(age) \sim 8.1$) were selected from the COCD. 24 objects were selected following these criteria. To extend the sample, another 9 open clusters were selected in the same coordinate range but with no previous age estimates.

Data were acquired during five nights in Jan. 1994 and ten nights in Jan. 1998 at the CTIO 0.9 m telescope. Due to technical difficulties (focus), and to some non photometric nights, only 30 clusters were observed. The typical seeing during both runs was about $1.2''$ although a few images presented higher values ($\sim 2.0''$). The cluster names, coordinates and observing run are presented in Table 1.

Table 1. Observed open clusters

Name	l	b	$\alpha(2000)$	$\delta(2000)$	Run
Bo 5	232.°57	+00.°69	$07^h30.^m9$	$-17°04'$	1998
Cz 29	230.°80	+00.°93	$07^h28.^m3$	$-15°24'$	1998
Haf 10	230.°82	+01.°00	$07^h28.^m6$	$-15°23'$	1998
Haf 16	242.°07	+00.°47	$07^h50.^m3$	$-25°27'$	1994
Haf 18	243.°11	+00.°42	$07^h52.^m5$	$-26°22'$	1994
Haf 19	243.°04	+00.°52	$07^h52.^m7$	$-26°15'$	1994
NGC 2302	219.°28	−03.°10	$06^h51.^m9$	$-07°04'$	1998
NGC 2309	219.°89	−02.°22	$06^h56.^m2$	$-07°12'$	1998
NGC 2311	217.°73	−00.°68	$06^h57.^m8$	$-04°35'$	1998
NGC 2335	223.°62	−01.°26	$07^h06.^m6$	$-10°05'$	1998
NGC 2343	224.°31	−01.°15	$07^h08.^m3$	$-10°39'$	1998
NGC 2353	224.°73	+00.°38	$07^h14.^m6$	$-10°18'$	1994
NGC 2367	235.°64	−03.°85	$07^h20.^m1$	$-21°56'$	1994
NGC 2383	235.°27	−02.°43	$07^h24.^m8$	$-20°56'$	1998
NGC 2384	235.°39	−02.°42	$07^h25.^m1$	$-21°02'$	1998
NGC 2401	229.°67	+01.°85	$07^h29.^m4$	$-13°58'$	1998
NGC 2414	231.°41	+01.°97	$07^h33.^m3$	$-15°27'$	1998
NGC 2425	231.°49	+03.°31	$07^h38.^m3$	$-14°52'$	1998
NGC 2432	235.°48	+01.°78	$07^h40.^m9$	$-19°05'$	1998
NGC 2439	246.°41	−04.°43	$07^h40.^m8$	$-31°39'$	1994
NGC 2453	243.°33	−00.°93	$07^h47.^m8$	$-27°14'$	1998
NGC 2533	247.°80	+01.°29	$08^h07.^m0$	$-29°54'$	1998
NGC 2571	249.°10	+03.°54	$08^h18.^m9$	$-29°44'$	1998
NGC 2588	252.°28	+02.°45	$08^h23.^m2$	$-32°59'$	1998
NGC 2635	255.°60	+03.°97	$08^h38.^m5$	$-34°46'$	1998
Rup 18	239.°94	−04.°92	$07^h24.^m8$	$-26°13'$	1998
Rup 55	250.°68	+00.°76	$08^h12.^m3$	$-32°36'$	94/98
Rup 72	259.°55	+04.°37	$08^h52.^m1$	$-37°36'$	1998
Rup 158	259.°55	+04.°42	$08^h52.^m3$	$-37°34'$	1998
Tr 7	238.°28	−03.°39	$07^h27.^m3$	$-24°02'$	94/98

In both runs, images were taken with a 2048×2048 Tek CCD and the standard set of *UBVRI* filters available at CTIO. The $0.39''$/pixel plate scale resulted in a field of view of $13' \times 13'$. Images were acquired using the CTIO ARCON operating in Quad mode (`http://www.ctio.noao.edu/instruments/arcon/arcon.html`). The gain was set at 3.2 e^-/adu and the readout noise was determined to be 4.0 e^-.

Besides the cluster fields, a number of standard star fields (Landolt 1983, 1992) were observed for calibration purposes. For the bias level and flat field corrections, zero second exposures and blank sky exposures in all filters were acquired each night. In the 1998 run, several short and long dome exposures were obtained with the purpose of creating a mask for the correction of shutter effects.

3. Data reduction

3.1. Photometry

Images were processed using IRAF. All images were subjected to the usual overscan, bias, and flatfield corrections. In the case of the 1998 run, a shutter mask was built and used to correct both flatfield and object frames from shutter timing effects, prior to flatfield division. The shutter mask was built and used following a variation of the recipe given by Stetson (1989) using six series of one twenty sec exposures and twenty one sec exposures. In the 1994 run no shutter images were acquired, so these data were not corrected from shutter effects. To quantify the effect of the shutter on the 1994 data we have analysed our photometry of Ruprecht 55 and Trumpler 7, which were observed on both runs, and found no significant trends.

Photometry was performed using the IRAF/DAOPHOT (Stetson et al. 1990) package. Standard stars were measured via aperture photometry with the APPHOT task. A 26 pix (10″) radius aperture was adopted since it included virtually all the stellar flux in all images as indicated by a growth curve analysis (Howell 1989). Magnitudes in the cluster fields were obtained following the standard procedures for PSF determination and fitting within IRAF/DAOPHOT. Due to the large size of the CCD chip, a quadratically variable PSF had to be used. About 60–70 well distributed PSF stars were selected by hand in each frame and were also used in the aperture correction determinations. The variable PSF was not able to adequately model the external regions of the images, so measurements for stars separated less than 150 pix from the edges were not used, which limited the useful field of view to $11' \times 11'$. Stars with a goodness of fit parameter, χ, greater that 2.5 and with error estimates greater than 0.1, as output from ALLSTAR, were also dropped out. At the end of this process a list of aperture corrected PSF photometry was obtained for each image. In total, 4.095 standard star aperture measurements and 2.096.414 cluster field PSF measurements were performed.

3.2. Atmospheric extinction

Although there are good reasons to determine the extinction and transformation coefficients simultaneously through a multilinear regression (Harris et al. 1981), our experience has shown us that the presence of a larger number of free parameters in each equation can affect the robustness of the method, thus leading to unphysical coefficients (such as negative extinction coefficients when airmass-colour cross terms are included). Therefore, we have decided to determine the extinction and transformation coefficients separately.

Traditionally, extinction is determined assuming Bouguer's law, $M_i = M_{i0} + K_i X$, where M_i is the i band magnitude measured at airmass X, M_{i0} is the magnitude one would measure outside the atmosphere, and K_i is the extinction coefficient for band i. Following this model, the extinction coefficient is usually determined as the slope yielded by a simple linear least squares fit of M_i vs. X. Ignoring the contribution of higher order extinction coefficients (Young 1974), the main inconvenience of this approach is that the slope determination should be based on many measurements of a single star. Since M_{i0} will be different from star to star one can not use different stars on a simultaneous determination of K_i in a direct manner. The use of an average K_i value determined from a few measurements of different stars is not a good alternative because the errors of individual determinations can be very large, producing an uncertain K_i. One way to use different stars in a simultaneous determination of the extinction coefficients is to employ Bouguer's law in a modified fashion. If we consider two measurements of a star at two different airmasses, we can write $\Delta M = K\Delta X$, were ΔM is the difference of the star's magnitudes measured at different airmasses and ΔX is the difference of the airmasses (the i index is dropped for simplicity). Since the M_0 term is no longer present, this equation is independent of the star under consideration and therefore measurements from different stars can be used in a simultaneous determination of the extinction coefficient. When there are N measurements at different airmasses for a certain star the question of which of the possible $N(N-1)/2$ differences, ΔM and ΔX, should be used arises, since only $N-1$ of them are independent. One of the most natural solutions would be to use the lowest airmass measurement as a reference to be subtracted from all the other measurements so that the range in ΔX would be maximised. The drawback of this choice is that any error in the reference's measurements will be introduced in a systematic way in all the differences. Since in principle any of the possible ΔM and ΔX could be used to determine the extinction coefficient, we have decided to use all the possible differences together in the same plot expecting that a *bad* measurement should produce outliers distinguishable from the dense cloud of *good* points.

Figure 1 shows the linear fits of the extinction determinations for the 1994 and 1998 runs. The fits were performed with the origin fixed to zero. A per night analysis showed that within each run the extinction coefficients remained constant (with a precision better that 0.01 mag), and therefore data from different nights were used together to determine average extinction coefficients for each run. The results are summarised in Table 2, where a noticeable decrease in extinction of about 0.03 mag is appreciated from 1994 to 1998.

3.3. Transformation to the standard system

Once the instrumental magnitudes were corrected from extinction, night to night variations in the instrumental zero point were determined, for each band, relative to a reference night (in the same observing run) using stars that were observed across several nights. These

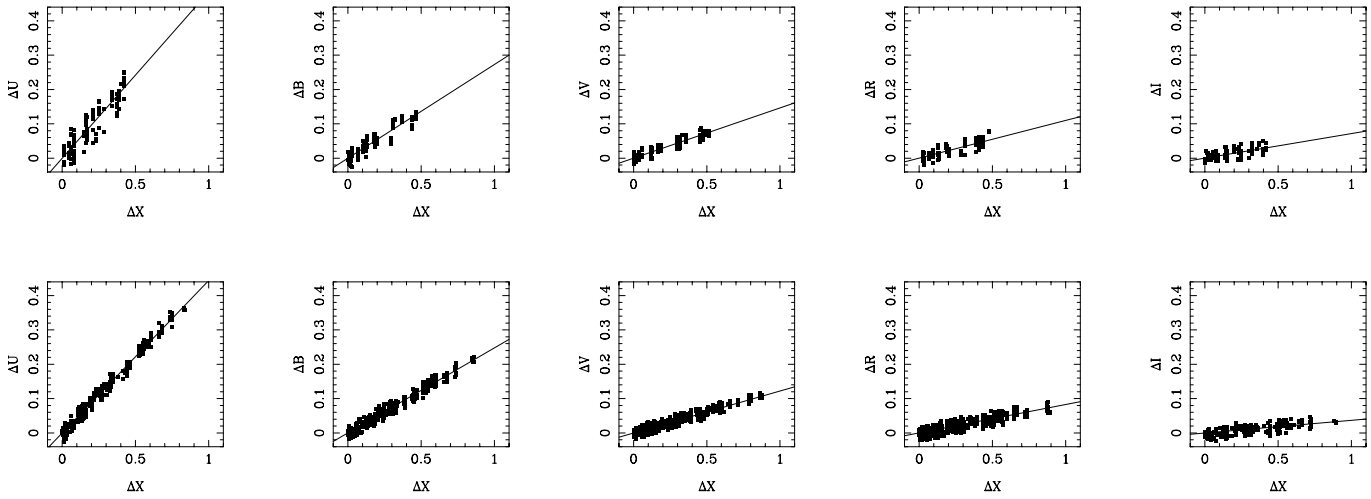

Fig. 1. Top: linear fits for the 1994 run extinction determinations. Bottom: the same for the 1998 run

Table 2. Extinction coefficients and rms residuals of the fits

Run	K_U	σ_U	K_B	σ_B	K_V	σ_V	K_R	σ_R	K_I	σ_I
1994	0.484	0.029	0.273	0.015	0.146	0.009	0.110	0.013	0.072	0.012
1998	0.444	0.012	0.248	0.011	0.122	0.008	0.083	0.010	0.037	0.009

displacements were used to transform observations from different nights onto the system of the reference night.

As previously mentioned, photometry for several stars from Landolt (1992) was obtained in order to determine the transformations between the instrumental and the standard system. We assume that the instrumentation was stable enough so that besides zero point variations, the transformation coefficients did not change within an observing run. The photometric relations between the reference night and the standard system were taken to be of the form of Eqs. (1) to (5).

$$v - V = \alpha_0 + \alpha_1(B - V) \quad (1)$$
$$(b - v) = \beta_0 + \beta_1(B - V) \quad (2)$$
$$(u - b) = \gamma_0 + \gamma_1(B - V) + \gamma_2(U - B) \quad (3)$$
$$(v - i) = \delta_0 + \delta_1(V - I) \quad (4)$$
$$(v - r) = \varepsilon_0 + \varepsilon_1(V - R). \quad (5)$$

In these equations, the upper case letters refer to the standard indexes, the lower case letters are the instrumental magnitudes and colours (corrected from atmospheric extinction and on the system of the reference night). The α_i, β_i, γ_i, δ_i, and ε_i were determined through least squares fits. In the 1998 data the residuals of the $(u - b)$ transformation (Eq. (3)) showed some dependence on $(B - V)^2$, so for this run Eq. (3) was modified to

$$(u - b) = \gamma_0 + \gamma_1(B - V) + \gamma_2(U - B) + \gamma_3(B - V)^2. \quad (6)$$

Because the B photometry was not as deep as the V photometry, Eq. (7) was used in the determination of the V magnitudes when B photometry was not available.

$$v - V = \zeta_0 + \zeta_1(V - I). \quad (7)$$

The transformation coefficients obtained from the linear fits of Eqs. (1) to (7) are presented in Table 3. This table also presents the zero point coefficients for each night corrected from the displacements relative to the reference night. The reference night for each run is marked with an asterisk. Coefficients for nights 6, 7 and 10 of the 1998 run are not presented since these were considered to be non photometric due to occasional cloud coverage. The rms deviations of the fits are shown in Table 4. In the 1994 run, typically 14 standard stars were observed each night, resulting in a total of 17 standards for the whole run. In the 1998 run about 30 standard stars were observed each night, yielding a total of 60 standards.

4. Construction of the photometric catalogue

The photometry lists obtained as described in Sect. 3.1 were corrected from atmospheric extinction using the coefficients in Table 2 and transformed to the system of the reference night. Since several measurements per band were available for each cluster, the final instrumental photometry is an average of the individual measurements weighted by the internal errors output by the ALLSTAR task. The final internal errors assigned to each star were taken to be the error of the average. When only one measurement was available the error was taken to be the one output by ALLSTAR. The average magnitudes were then transformed to the standard system using the coefficients from Table 3.

As previously mentioned, nights 6, 7 and 10 of the 1998 run were considered non photometric due to occasional cloud coverage. During the clear periods of these nights, long exposures of several open clusters were

Table 3. Transformation coefficients

Run	Night	α_0	α_1	β_0	β_1	γ_0	γ_1	γ_2	γ_3	δ_0	δ_1	ε_0	ε_1	ζ_0	ζ_1
1994	1	2.821	−0.013	0.148	1.106	1.625	0.076	0.757	0.000	−1.000	0.997	−0.128	0.963	2.821	−0.012
	2	2.801	−0.013	0.162	1.106	1.559	0.076	0.757	0.000	−1.015	0.997	−0.126	0.963	2.801	−0.012
	3	2.832	−0.013	0.185	1.106	1.635	0.076	0.757	0.000	−0.995	0.997	−0.121	0.963	2.832	−0.012
	4*	2.839	−0.013	0.180	1.106	1.614	0.076	0.757	0.000	−0.976	0.997	−0.111	0.963	2.840	−0.012
	5	2.844	−0.013	0.180	1.106	1.597	0.076	0.757	0.000	−0.950	0.997	−0.100	0.963	2.845	−0.012
1998	1	2.826	−0.015	0.185	1.096	1.480	−0.013	0.772	0.144	−0.994	0.999	−0.124	0.964	2.830	−0.017
	2	2.821	−0.015	0.167	1.096	1.503	−0.013	0.772	0.144	−1.004	0.999	−0.115	0.964	2.825	−0.017
	3*	2.825	−0.015	0.175	1.096	1.500	−0.013	0.772	0.144	−1.003	0.999	−0.115	0.964	2.828	−0.017
	4	2.815	−0.015	0.174	1.096	1.497	−0.013	0.772	0.144	−1.008	0.999	−0.122	0.964	2.819	−0.017
	5	2.811	−0.015	0.175	1.096	1.506	−0.013	0.772	0.144	−1.009	0.999	−0.115	0.964	2.815	−0.017
	8	2.767	−0.015	0.166	1.096	1.491	−0.013	0.772	0.144	−1.009	0.999	−0.119	0.964	2.770	−0.017
	9	2.754	−0.015	0.176	1.096	1.485	−0.013	0.772	0.144	−1.021	0.999	−0.112	0.964	2.758	−0.017

Table 4. Rms residuals of the transformations to the standard system

Run	ΔV (Eq. (1))	$\Delta(B-V)$ (Eq. (2))	$\Delta(U-B)$ (Eq. (3))	$\Delta(V-I)$ (Eq. (4))	$\Delta(V-R)$ (Eq. (5))	ΔV (Eq. (7))
1994	0.011	0.012	0.024	0.016	0.011	0.011
1998	0.012	0.008	0.010	0.007	0.007	0.012

acquired (NGC 2571, NGC 2311, NGC 2343, NGC 2432, NGC 2635, and Rup 18). The photometry for these frames was then transformed to the instrumental system by comparison with shorter exposures taken on photometric nights.

The final catalogue of calibrated data which includes photometry and error estimates for 64.619 stars in at least three of the five *UBVRI* bands will be made available electronically at the CDS. Table 5 summarises the contribution in number of measurements, photometric depth and field of view of this study relative to previous works. In Table 5, N is the number of stars measured in this work, $N_{\rm O}$, $V_{\rm lim}$ and *Field* are the number of stars, limiting magnitude and the field of view covered in previous works that used the technique presented in the *Data* column (pe – photoelectric; pgr – photographic; ccd – CCD). The column *Other* indicates the existence of other studies performed using other techniques that, due their lower precision or number of stars, were not included in the comparison. For this work the limiting magnitude is $V_{\rm lim} \sim 21$ (except for Haf 18 and Haf 19 where $V_{\rm lim} \sim 20$) and the field of view is approximately $11' \times 11'$. In Table 5, the clusters marked with the same symbol have small angular separations and appear in the same image. For these clusters the number of stars refers to the whole image and is indicated only once. All the other empty fields represent unavailable data. The data from previous studies was obtained from the WEBDA (`http://obswww.unige.ch/webda/`) open cluster database of Mermilliod (1988, 1992). The WEBDA database has allowed this and other analysis throughout this work to be performed in a reasonable time.

5. Photometric errors

The path that leads from the observations to the final calibrated photometry is composed of several steps, each one affected by some error that contributes to the total uncertainty of the final results. To estimate the errors we have split the problem in two parts. In the first place are all the processes involved in obtaining the instrumental magnitudes, which are mainly affecting the photometric precision. In the second place is the transformation to the standard system, which mainly affects the final photometric accuracy.

In the process of arriving to the instrumental magnitudes, CCD images were processed, PSFs were fit, aperture and extinction corrections were applied, and night to night photometric zero point offsets were also applied. The whole process is highly complex and full of subjective decisions, which makes any formal step by step error treatment virtually impossible. Nevertheless, we can analyse how the these processes affect the photometric precision by analysing the dispersion of measurements.

Figure 2 shows the standard deviation (not the error of the mean value) of the instrumental magnitudes for stars in the field of NGC 2571 which have 10 or more measurements and therefore represent the error of an individual measurement. Table 6 summarises the data in Fig. 2 for a number of magnitude ranges.

Because NGC 2571 was observed in four different nights, the dispersion also includes the effects of uncertainties in the night to night variations of the transformation zero point. The errors of the averaged data are represented by the error of the mean which are smaller than values in Table 6, depending on the number of measurements

Table 5. Contribution of this study relative to previous work. For this study $V_{\rm lim} \sim 21$ and the field of view is $11' \times 11'$

Cluster	N	$N_{\rm O}$	$V_{\rm lim}$	Field ($'$)	Data	Other
Bo 5	861	16	12.5	10×5	pe	
Cz 29[a]	3018	18	15	3×3	pgr	
Haf 10[a]		9	15	3×3	pgr	
Haf 16	4522	15	15	4×4	pe	
Haf 18[b]	2304	50	17	2×3	ccd	pe, pgr
Haf 19[b]		70	18	2×3	ccd	pe, pgr
NGC 2302	1521	16	15	4×4	pe	
NGC 2309	1767		21	6×6	ccd	
NGC 2311	1191					
NGC 2335	1332	60	14	20×20	pe	
NGC 2343	1319	55	15	16×16	pe	
NGC 2353	2199	53	15	17×17	pe	pgr
NGC 2367	2571	15	14	3×4	pe	
NGC 2383[c]	2682	722	20.5	5×5	ccd	pe
NGC 2384[c]		304	20	5×5	ccd	pe
NGC 2401	1892					
NGC 2414	1992	12	14	4×3	pe	pgr
NGC 2425	2397					
NGC 2432	2901					
NGC 2439	3477	120	18.5	2×3	ccd	pe, pgr
NGC 2453	2605	356	19	4×6	ccd	pe, pgr
NGC 2533	3121	122	14.5	11×11	pgr	pe
NGC 2571	2723	144	14.5	16×16	pgr	pe
NGC 2588	2904					
NGC 2635	3198	6	14	2×2	pe	
Rup 18	2068	20	14	2×7	pe	
Rup 55	4534	29	16	4×4	pe	pgr
Rup 72[d]	2951					
Rup 158[d]						
Tr 7	2569	16	14	3×5	pe	

Table 6. Typical precision of an individual measurement

V	σ_U	σ_B	σ_V	σ_R	σ_I
$\leq$14	0.026	0.015	0.011	0.012	0.012
14−16	0.033	0.021	0.017	0.016	0.018
16−18	0.042	0.038	0.032	0.026	0.031
>18	—	0.054	0.053	0.046	0.043

used. Most stars in the catalogue have three measurements per band, although there are cases like NGC 2571 and Rup 18 that have been observed up to seventeen times per band and whose errors are considerably smaller (about one fourth of the tabulated values).

The total photometric errors for a single measurement have been estimated by quadratically adding the internal errors from Table 6 to obtain the errors in each colour and then quadratically adding these errors to the residuals of the standard transformation from Table 3. The total errors are presented in Table 7. The values in this table should be regarded as upper error limits for our photometry since they refer to individual measurements. Also, when constructing the colour indexes some contributions to the magnitude errors tend to cancel out instead of increasing the uncertainty, as we have assumed by quadratically adding the errors in each band. Finally, because only one long exposure per band was acquired for NGC 2571, the error analysis has been performed using photometry from short exposure frames, therefore leading to overestimated errors in the faint end.

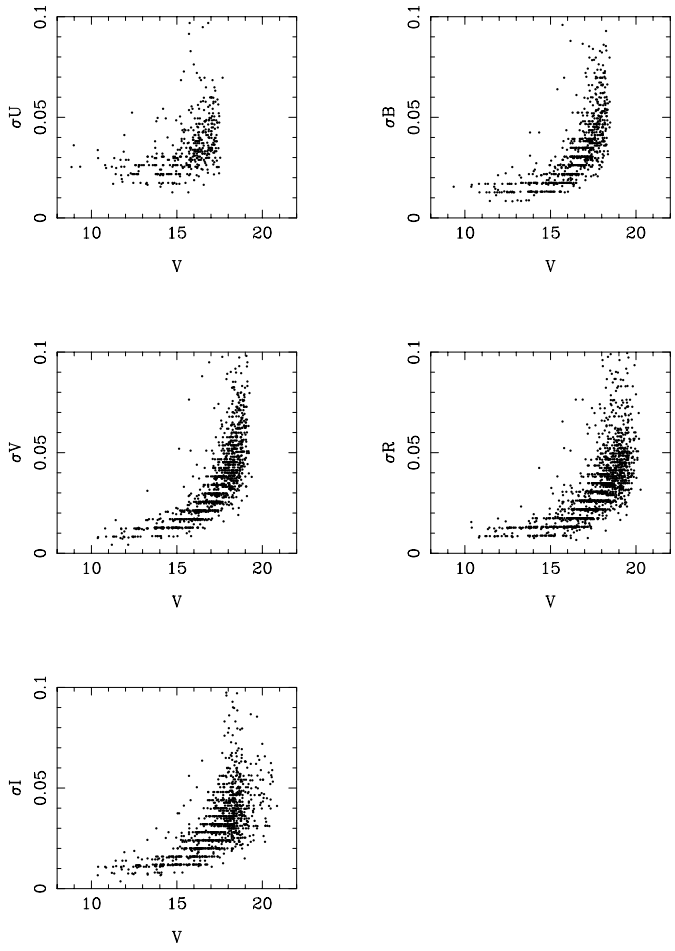

Fig. 2. Standard deviation of the instrumental magnitudes for stars of NGC 2571 observed 10 times or more

Table 7. Total errors for individual measurements

V	σ_V	$\sigma_{(B-V)}$	$\sigma_{(U-B)}$	$\sigma_{(V-R)}$	$\sigma_{(V-I)}$
$\leq$14	0.016	0.020	0.032	0.018	0.018
14−16	0.021	0.028	0.040	0.024	0.026
16−18	0.034	0.050	0.058	0.042	0.045
>18	0.054	0.076	—	0.071	0.069

6. Comparison with photometry from other studies

Several of the observed cluster fields have been the subject of previous photometric studies. Most of them, however, have been performed by different authors using different kinds of detectors, filters, and sets of standard stars. The comparison of these data to the homogeneous photometry from this study can provide a common photometric scale therefore making the discussion of the different results more meaningful. In the search of photometry and finding charts from previous studies we have made extensive use of the WEBDA database. The result of the comparisons is summarised in Table 8 where only studies with more than five stars in common were considered.

In Tables 8a and 8b, Δ is the difference between our photometry and previous one in the sense of $\Delta =$ *this work* – *previous work*, σ is the standard deviation of Δ, N is the number of stars used in the comparison, and *Data* is the kind of compared data: *Pe* – photoelectric, *Pgr* – photographic, and *CCD* – CCD. Because of the large number of studies involved, we have limited the analysis to the average differences and their dispersions. Some stars that presented large discrepancies possibly due to bad identifications, variability, or contamination from neighbouring stars (affecting non-psf studies) were not used.

The comparisons in Tables 8a and 8b show that in general our photometry does agree with the one from other studies. Cases were the agreement is not so good usually correspond to comparisons with photographic data (ex. Cz 29 and Haf 10). There are significative differences relative to the photoelectric photometry of Seggewiss (1971), but there is good agreement with other data for the same clusters.

In the case of Haf 19 we find a great difference in $(U-B)$ relative to the values of Munari & Carraro (1996) ($\Delta(U-B) \sim -0.3$). On the other hand we find that our $(U-B)$ photometry is comprised between the data of Moffat & FitzGerald (1974a) and FitzGerald & Moffat (1974), although the dispersion in these comparisons is quite large ($\sigma \sim 0.1$). The photometry of NGC 2635 also presents large deviations from the one obtained by Vogt & Moffat (1972). However the comparison was performed with only five stars, and three of them have very close bright neighbours, which could be the explanation of the higher brightness of the photoelectric data of Vogt & Moffat (1972) relative to our PSF magnitudes.

Regarding the *VRI* comparisons, we find good agreement with the CCD photometry of Munari & Carraro (1996) and Munari et al. (1998), and somewhat large deviations with respect to the $(V-I)$ colours from the other CCD studies. The largest deviations occur with the photoelectric data of Jorgensen & Westerlund (1988) where the difference is better described by a significative colour term $(\Delta(V-R)_{\rm pe} = 0.009 - 0.621 \times (V-R)_{\rm CCD}$ with $\sigma \sim 0.052$; and $\Delta(V-I)_{\rm pe} = 0.008 - 0.437 \times (V-I)_{\rm CCD}$ with $\sigma \sim 0.194$).

7. Interstellar extinction

In this section we discuss the extinction law in the direction of our open cluster sample. We find that the typical Galactic values for the reddening slope, $E(U-B)/E(B-V) = 0.72$, and for the ratio of total to selective absorption, $R_V \sim 3.1$, are consistent with our data. The adopted values for the reddening slope, the ratio of total to selective absorption will be used in the subsequent papers of this series to correct our data from the effects of interstellar extinction.

7.1. The reddening slope

Determining the amount of interstellar reddening from photometry alone using techniques such as ZAMS main sequence fitting in a colour-colour diagram, or Johnson & Morgan's (1953) *Q Method*, requires the knowledge of the slope of the reddening line. It is well known (Mathis 1990; Turner 1994) that there are variations in the reddening law throughout the Galaxy, although a mean reddening slope of $E(U-B)/E(B-V) = 0.72$ is found for most Galactic longitudes.

Turner (1989) in an empirical study of the fields of six open clusters determined a mean value of $E(U-B)/E(B-V) = 0.724 \pm 0.005$ for the reddening slope, although values ranging from at least 0.62 to 0.80 were found from one region to another. One of the regions analysed by Turner (1989) was the field of NGC 2439, which is also one of the clusters in our sample, and for which he finds a value of $E(U-B)/E(B-V) = 0.75$.

To investigate the reddening law in the region of our open cluster sample we have searched the WEBDA database for MK spectral types of O, B, A dwarfs observed in this study in order to derive their intrinsic colours. The intrinsic colours were determined by interpolation over the tables given by Schmidt-Kaler (1982) which relate MK types to the *UBV* indexes and were then used to compute the colour excesses.

Figure 3 shows the linear fit to the slope of the colour excess data. The fit yielded a value of $(E(U-B)/E(B-V) = 0.69 \pm 0.03$ with an 0.07 rms dispersion of the residuals, which despite its low accuracy is in excellent agreement with the *standard* slope of 0.72. The relatively high dispersion in the residuals may be due to errors in the spectral classifications (as suggested by the dispersion of the NGC 2453 data) and do not necessarily reflect to cluster to cluster variations of the reddening law. In view of these results we find that the reddening law in the direction of our sample follows the mean Galactic law and we therefore adopt the standard value $E(U-B)/E(B-V) = 0.72$ for subsequent reddening analysis. For the other colour-colour combinations, the standard slopes given by Straižys (1992) were adopted. We do note however that the available data is not sufficient for a rigorous analysis, so that cluster to cluster variations up to $\sim$0.07 in the reddening slope cannot be discarded.

Table 8. a) Comparison with previous *UBV* photometry

Cluster	ΔV	σ	N	$\Delta(B-V)$	σ	N	$\Delta(U-B)$	σ	N	Data	Ref
Bo 5	0.025	0.017	11	0.000	0.025	14	−0.006	0.038	9	pe	1
Cz 29	0.179	0.142	18	0.073	0.056	14	−0.025	0.104	15	pgr	2
Haf 10	0.284	0.244	9	0.087	0.142	8	−0.046	0.183	7	pgr	2
Haf 16	0.030	0.090	12	0.020	0.054	11	0.087	0.041	11	pe	3
Haf 18	0.030	0.090	20	0.075	0.050	20	0.022	0.154	22	pgr	4
Haf 18	0.047	0.048	14	0.000	0.038	13	−0.044	0.046	11	pe	5
Haf 18	−0.002	0.016	50	−0.042	0.017	51	0.046	0.091	10	ccd	6
Haf 18	−0.012	0.029	26	−0.035	0.030	23	—	—	—	ccd	7
Haf 19	0.024	0.015	50	−0.092	0.017	52	−0.308	0.045	11	ccd	8
Haf 19	0.027	0.063	16	0.056	0.077	20	−0.042	0.108	16	pe	5
Haf 19	−0.010	0.073	17	0.099	0.081	19	0.042	0.146	20	pgr	4
Haf 19	−0.015	0.018	31	−0.048	0.021	31	—	—	—	ccd	7
NGC 2302	0.061	0.062	15	−0.005	0.014	13	0.032	0.049	14	pe	1
NGC 2335	0.027	0.022	24	−0.013	0.016	24	−0.005	0.046	24	pe	9
NGC 2335	0.163	0.087	5	0.029	0.030	5	−0.075	0.069	5	pe	10
NGC 2343	0.055	0.034	32	−0.011	0.015	33	−0.005	0.040	36	pe	11
NGC 2343	0.164	0.116	7	0.000	0.026	6	0.010	0.143	7	pe	10
NGC 2353	−0.028	0.031	23	−0.003	0.026	25	−0.027	0.093	26	pe	12
NGC 2353	−0.026	0.071	57	0.000	0.069	59	0.006	0.105	53	pgr	13
NGC 2353	−0.061	0.043	5	0.030	0.062	5	−0.006	0.089	5	pe	13
NGC 2353	−0.031	0.145	4	0.008	0.020	4	−0.028	0.147	4	pe	14
NGC 2367	0.013	0.032	12	−0.010	0.011	11	−0.065	0.041	12	pe	3
NGC 2367	−0.033	0.012	6	−0.009	0.043	8	−0.035	0.013	5	pe	15
NGC 2383	−0.014	0.018	8	0.035	0.038	11	−0.009	0.068	9	pe	3
NGC 2383	0.000	0.054	579	−0.014	0.066	487	—	—	—	ccd	16
NGC 2384	0.033	0.025	10	0.036	0.020	10	0.000	0.021	10	pe	3
NGC 2384	0.052	0.051	19	0.021	0.034	20	−0.009	0.031	14	pgr	17
NGC 2384	0.041	0.060	215	0.006	0.066	185	—	—	—	ccd	16
NGC 2414	0.019	0.035	7	−0.007	0.016	7	—	—	—	pe	3
NGC 2439	−0.007	0.041	98	0.004	0.029	95	0.026	0.107	92	pgr	18
NGC 2439	0.002	0.027	96	−0.022	0.042	89	−0.032	0.061	33	ccd	19
NGC 2439	−0.003	0.027	38	−0.013	0.022	39	0.031	0.047	34	pe	18
NGC 2439	−0.060	0.106	48	−0.024	0.059	47	—	—	—	pgr	20
NGC 2453	0.001	0.056	44	0.061	0.069	43	−0.108	0.060	36	pgr	21
NGC 2453	0.016	0.042	16	−0.004	0.026	16	−0.046	0.054	20	pe	22
NGC 2453	0.037	0.039	292	0.028	0.046	180	—	—	—	ccd	23
NGC 2453	0.105	0.125	5	0.059	0.045	6	−0.060	0.078	6	pe	10
NGC 2533	−0.004	0.090	93	0.120	0.092	93	0.192	0.074	37	pgr	24
NGC 2533	0.020	0.084	5	−0.024	0.047	4	0.011	0.042	4	pe	25
NGC 2533	0.054	0.034	7	−0.038	0.034	7	0.030	0.022	6	pe	26
NGC 2533	−0.041	0.041	11	−0.021	0.039	13	−0.080	0.061	12	pe	27
NGC 2571	0.002	0.025	37	−0.013	0.015	38	−0.007	0.038	39	pe	28
NGC 2571	0.098	0.069	73	−0.011	0.068	70	−0.014	0.072	71	pgr	29
NGC 2571	−0.008	0.099	76	0.050	0.150	84	−0.048	0.131	40	pgr	24
NGC 2635	0.159	0.114	6	0.029	0.077	5	−0.097	0.233	6	pe	3
Rup 18	0.011	0.042	19	0.023	0.017	16	−0.135	0.094	18	pe	1
Rup 55	0.009	0.032	13	−0.020	0.031	14	−0.035	0.058	13	pe	1
Tr 7	0.029	0.021	6	0.016	0.020	6	−0.034	0.048	6	pe	3

Table 8. b) Comparison with previous *VRI* photometry

Cluster	$\Delta(V-R)$	σ	N	$\Delta(V-I)$	σ	N	Data	Ref
Haf 18	−0.001	0.012	35	0.033	0.027	33	ccd	6
Haf 19	0.028	0.020	57	0.015	0.019	55	ccd	8
NGC 2383	0.003	0.052	591	−0.095	0.061	564	ccd	16
NGC 2384	0.021	0.057	223	−0.103	0.080	224	ccd	16
NGC 2453	—	—	—	0.061	0.056	287	ccd	23
NGC 2533	−0.118	0.204	11	−0.289	0.318	15	pe	27

References for Tables 8a and 8b

1 — Moffat & Vogt (1975)
2 — FitzGerald & Moffat (1980)
3 — Vogt & Moffat (1972)
4 — FitzGerald & Moffat (1974)
5 — Moffat & FitzGerald (1974a)
6 — Munari et al. (1998)
7 — Labhart et al. (1992)
8 — Munari & Carraro (1996)
9 — Clariá (1973)
10 — Seggewiss (1971)
11 — Clariá (1972)
12 — FitzGerald et al. (1990)
13 — Hoag et al. (1961)
14 — Clariá (1974)
15 — Pedreros (1984)
16 — Subramaniam & Sagar (1999)
17 — Hassan (1984)
18 — White (1975)
19 — Ramsay & Pollaco (1992)
20 — Becker et al. (1976)
21 — Moffat & FitzGerald (1974b)
22 — Moffat & FitzGerald (1974b)
23 — Mallik et al. (1995)
24 — Lindoff (1968)
25 — Eggen (1974)
26 — Havlen (1976)
27 — Jorgensen & Westerlund (1988)
28 — Clariá (1976)
29 — Kilambi (1978)

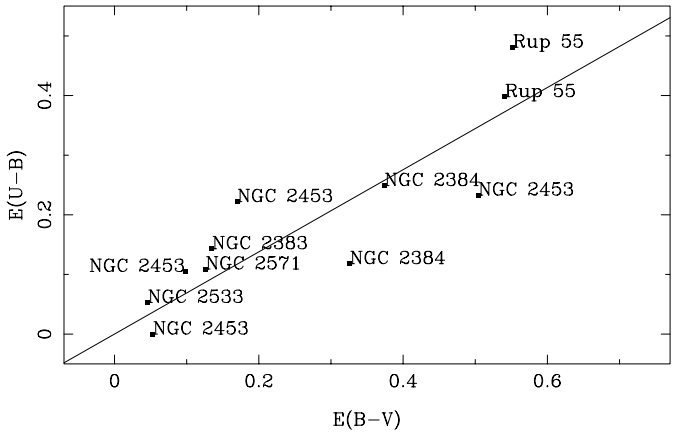

Fig. 3. Reddening slope defined by the data of the 1998 run. The straight line is a fit of $E(U-B)/E(B-V) = 0.69 \pm 0.03$ with an 0.07 rms dispersion of the residuals

7.2. The ratio of total to selective absorption

As in the case of the reddening slope, it is not possible to perform a rigorous study of the ratio of total to selective absorption, $R_V = A_V/E(B-V)$, where A_V is the absorption in the V band. The same kind of proportionality is also defined for the other combinations of bands and colours. Several authors (Sherwood 1975; Crawford & Mandwewala 1976; Turner 1976) have shown that the ratio of total to selective absorption has a typical value of $R_V \sim 3.1$ for a diffuse interstellar medium. Denser molecular clouds can give rise to higher values of R_V around 4−6 (Mathis 1990; Turner 1994).

For cases in which there is evidence of variable extinction across a cluster field, where all cluster members are assumed to be at a common distance, a plot of $V - M_V$ versus $E(B-V)$ should show a correlation of slope R_V. Evidently, this method commonly known as the *variable extinction method* requires the knowledge of the absolute magnitude, M_V, and the colour excess, $E(B-V)$, for each star. Both M_V and $E(B-V)$ can be derived from spectral types. Turner (1976) applied this method to determine R_V for 51 open clusters and obtained an average value of $R_V = 3.08 \pm 0.03$. Three of the open clusters studied by Turner (1976) were NGC 2323, NGC 2343 and Trumpler 9, which lie in the same Galactic longitude range of our sample, and for which he obtained the values 2.85, 3.09 and 2.75 respectively.

We have also investigated the ratio of total to selective absorption using the same photometric and spectroscopic data as in the study of the reddening slope. Because there are not enough stars with known spectral types in each cluster, the variable extinction method cannot be used in a direct form. Instead, a differential approach, similar to the one in Sect. 3.2 for the determination of the

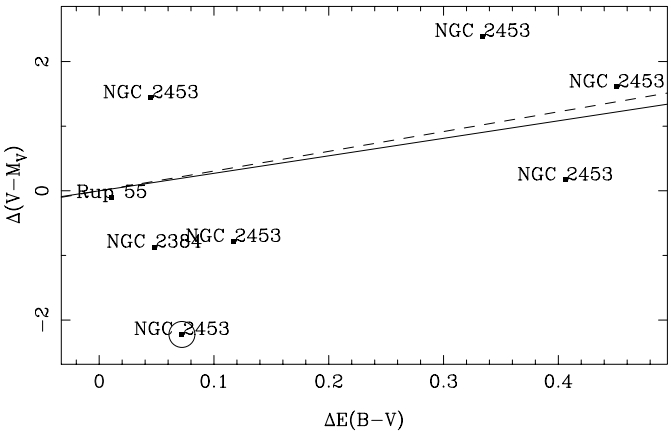

Fig. 4. The linear least squares fit of the slope yields $R_V = 2.71 \pm 0.70$. If the deviated point of NGC 2453 (marked with a circle) is eliminated the fit yields $R_V = 3.06 \pm 0.75$

extinction coefficients, was followed. If a certain cluster has at least two stars with known spectral types we can write $\Delta(V - M_V) = R_V \Delta(E - B)$ which is distance independent and where R_V is the only unknown. Another advantage of this approach is that a greater range in $E(B - V)$ may be achieved than in the traditional one-cluster method. However, the sensitivity to cluster-to-cluster variations is lost and only an average value can be determined.

Figure 4 shows a plot of $\Delta(V - M_V)$ versus $\Delta(E - B)$. A value of $R_V = 2.71 \pm 0.70$ was found from a linear least squares fit of the slope (i.e. $\Delta(V - M_V) = 0$ for $\Delta(E - B) = 0$) which despite its large uncertainly is consistent with the *standard* $R_V = 3.1$. Furthermore, if the deviating point of NGC 2453 in the lower left of Fig. 4 is eliminated, then the fit yields $R_V = 3.06 \pm 0.75$ which is practically identical to the mean value of $R_V = 3.08$ given by Turner (1976). Once again, we take the value obtained in this analysis more as an indication that the region under study follows a standard extinction law than that an actual determination of R_V, and will use the standard $R_V = 3.1$ value in the upcoming analysis of our open cluster photometry.

8. Conclusions

We have obtained homogeneous *UBVRI* photometry in the fields of 30 open clusters between $217° < l < 260°$ and $-5° < b < 5°$ using data gathered at the same telescope, following the same reduction procedures, and calibrating all the data to the same *UBVRI* standard system. These data have resulted in a precise and deep (up to $V \sim 21$), photometric catalogue of approximately 65 000 stars.

We have compared our data to photometry from other sources finding that in general there is good agreement (at a 0.03 mag level) although some studies present large deviations. The differences between our photometry and that from other studies have been presented in a table which can be used to put all the measurements on the common scale defined by this study.

Since we intend to use this catalogue for cluster reddening, distance and age determinations, we have performed a rough analysis of the reddening slope and of the ratio of total to selective absorption for this region of the Galaxy and found that the typical Galactic values $E(U - B)/E(B - V) = 0.72$ and $R_V \sim 3.1$ are consistent with our data.

Acknowledgements. The author wishes to thank E. J. Alfaro and A. J. Delgado for providing the 1994 images. The author would also like to thank J.-C. Mermilliod and J. Alves for many useful comments and help. This work was financially supported by FCT (Portugal) through the grant PRAXIS XXI BD/3895/94 and the YALO project. Most of the work was done at the IAA-CSIC (Spain) as part of the author's Ph.D. research. This research made use of the NASA Astrophysics Data System, and of the Simbad database operated at the Centre de Données Stellaires – Strasbourg, France.

References

Alfaro, E. J., Cabrera-Caño, J., & Delgado, A. J. 1991, ApJ, 378, 106
Becker, W., Svolopoulos, S. N., & Fang, C. 1976, Sep. Astron. Inst, Univ. Basel, 89
Bessel, M. S. 1995, PASP, 107, 672
Carraro, G., Ng, Y. K., & Portinari, L. 1998, MNRAS, 296, 1045
Clariá, J. J. 1972, AJ, 77, 868
Clariá, J. J. 1973, A&AS, 9, 251
Clariá, J. J. 1974, AJ, 79, 1022
Clariá, J. J. 1976, PASP, 88, 225
Crawford, D. L., & Mandwewala, N. 1976, PASP, 88, 917
Dambis, A. K. 1998, AstL, 25, 10
Eggen, O. J. 1974, PASP, 86, 960
FitzGerald, M. P., Harris, G. L. H., & Reed, B. C. 1990, PASP, 102, 865
FitzGerald, M. P., & Moffat, A. F. J. 1974, AJ, 79, 873
FitzGerald, M. P., & Moffat, A. F. J. 1980, PASP, 92, 489
Harris, W. E., Fitzgerald, M. P., & Reed, B. C. 1981, PASP, 93, 507
Hassan, S. M. 1984, Astronomy with Schmidt-type telescope, 295
Havlen, R. J. 1976, A&A, 49, 307
Hoag, A. A., Johnson, H. L., Iriarte, B., et al. 1961, PUSNO, 17, 343
Howell, S. B. 1989, PASP, 101, 616
Janes, K. A., & Adler, D. 1982, ApJS, 49, 425
Johnson, H. L., & Morgan, W. W. 1953, ApJ, 117, 113
Jorgensen, U. G., & Westerlund, B. E. 1988, A&AS, 72, 193
Kilambi, G. C. 1978, PASP, 90, 721
Labhart, L., Spaenhauer, A., & Schwengeler, H. 1992, A&A, 265, 869
Landolt, A. U. 1983, AJ, 88, 439
Landolt, A. U. 1992, AJ, 104, 340
Lindoff, U. 1968, ArA, 4, 587
Loktin, A. V., & Matkin, N. V. 1994, Astron. Astrophys. Trans., 4, 153
Lyngå, G. 1981, Computer Based Catalogue of Open Cluster Data, Tech. rep., Observatoire de Strasbourg, Centre de Données Stellaires, Strasbourg
Lyngå, G. 1987, Computer Based Catalogue of Open Cluster Data, 5th ed., Tech. rep., Observatoire de Strasbourg, Centre de Données Stellaires, Strasbourg

Mallik, D. C. V., Sagar, R., & Pati, A. K. 1995, A&AS, 114, 537
Mathis, J. S. 1990, ARA&A, 28, 37
Mermilliod, J. C. 1988, Bull. Inform. CDS, 35, 77
Mermilliod, J. C. 1992, Bull. Inform. CDS, 40, 115
Moffat, A. F. J., & FitzGerald, M. P. 1974a, A&A, 34, 291
Moffat, A. F. J., & FitzGerald, M. P. 1974b, A&AS, 18, 19
Moffat, A. F. J., & Vogt, N. 1975, A&AS, 20, 85
Munari, U., & Carraro, G. 1996, MNRAS, 283, 905
Munari, U., Carraro, G., & Barbon, R. 1998, MNRAS, 297, 867
Pedreros, M. H. 1984, Ph.D. Thesis, University of Toronto, Toronto, Canada
Ramsay, G., & Pollacco, D. L. 1992, A&AS, 94, 73
Schmidt-Kaler, T. 1982, Stars and Star Clusters (Berlin: Springer), 15
Seggewiss, W. 1971, VeBon, 83, 19
Sherwood, W. A. 1975, Ap&SS, 34, 3
Stetson, P. B. 1989, Highlights Astron., 8, 635
Stetson, P. B., Davis, L. E., & Crabtree, D. R. 1990, in ASP Conf. Ser. 8: CCDs in Astronomy, 289
Straižys, V. 1992, Multicolor Stellar Photometry (Tucson: Pachart), 302
Subramaniam, A., & Sagar, R. 1999, AJ, 117, 937
Turner, D. G. 1976, AJ, 81, 1125
Turner, D. G. 1989, AJ, 98, 2300
Turner, D. G. 1994, RMxAA, 29, 163
Twarog, B. A., Ashman, K. M., & Anthony-Twarog, B. J. 1997, AJ, 114, 2256
Vogt, N., & Moffat, A. F. J. 1972, A&AS, 7, 133
White, S. D. M. 1975, ApJ, 197, 67
Young, A. T. 1974, Meth. Exp. Phys., 12A, 123